



DOI: [10.29026/oea.2024.240064](https://doi.org/10.29026/oea.2024.240064)

# Stimulated Raman scattering microscopy with phase-controlled light focusing and aberration correction for rapid and label-free, volumetric deep tissue imaging

Weiqli Wang and Zhiwei Huang<sup>ID</sup>\*

<sup>1</sup>Optical Bioimaging Laboratory, Department of Biomedical Engineering, College of Design and Engineering, National University of Singapore, Singapore 117576.

\*Correspondence: ZW Huang, E-mail: [biehzw@nus.edu.sg](mailto:biehzw@nus.edu.sg)

## This file includes:

[Section 1: System aberrations correction with Zernike polynomials in PC-SRS by using two-photon fluorescence \(TPF\) imaging of 500 nm fluorescent beads](#)

[Section 2: Relationship between the axial position of the excitation beam and the phase modulation in PC-SRS](#)

[Section 3: Length of the Bessel pump beam in PC-SRS obtained by using TPF imaging on 500 nm fluorescent beads](#)

[Media for supporting content](#)

Supplementary information for this paper is available at <https://doi.org/10.29026/oea.2024.240064>



**Open Access** This article is licensed under a Creative Commons Attribution 4.0 International License.

To view a copy of this license, visit <http://creativecommons.org/licenses/by/4.0/>.

© The Author(s) 2024. Published by Institute of Optics and Electronics, Chinese Academy of Sciences.

## Section 1: System aberrations correction with Zernike polynomials in PC-SRS by using two-photon fluorescence (TPF) imaging of 500 nm fluorescent beads

Three types of aberrations (oblique astigmatism, vertical astigmatism, and spherical) are corrected in PC-SRS by using Zernike polynomials (corresponding to  $Z_5$ ,  $Z_6$ ,  $Z_{11}$  (Noll index), respectively). The coefficients of these Zernike polynomials ranging from  $-2$  to  $2$  in  $0.2$  steps are used to the generation of 21 phase patterns for each Zernike polynomial. The phase patterns are varied on SLM for TPF imaging of fluorescent beads. The maximum TPF intensity of the fluorescent bead is set as criterion to select the optimal coefficient for the specific Zernike polynomial used. The merged phase patterns of these Zernike polynomials with optimized coefficients will be employed in PC-SRS imaging.

Figure S1(a, b) display the TPF image of 500 nm fluorescent bead captured with pump beam (800 nm) in  $x$ - $y$  plane corresponding to the conditions of the aberration corrections (AC-ON) and the absence of aberration corrections (AC-OFF). Figure S1(c) shows the intensity distribution of fluorescent bead along the dashed line in (a–b), giving rise to a  $\sim 1.75$ -fold enhancement of SNRs after the AC-ON for pump beam excitation. Figure S1(d–e) present the TPF image of 500 nm fluorescent bead captured by Stokes beam (1041 nm) in  $x$ - $y$  plane in the condition of AC-ON and AC-OFF. Figure S1(f) reveals the intensity distribution of fluorescent bead along the dashed line in (d–e), yielding a  $\sim 1.8$ -fold improvement of SNRs after the AC-ON for Stokes beam.

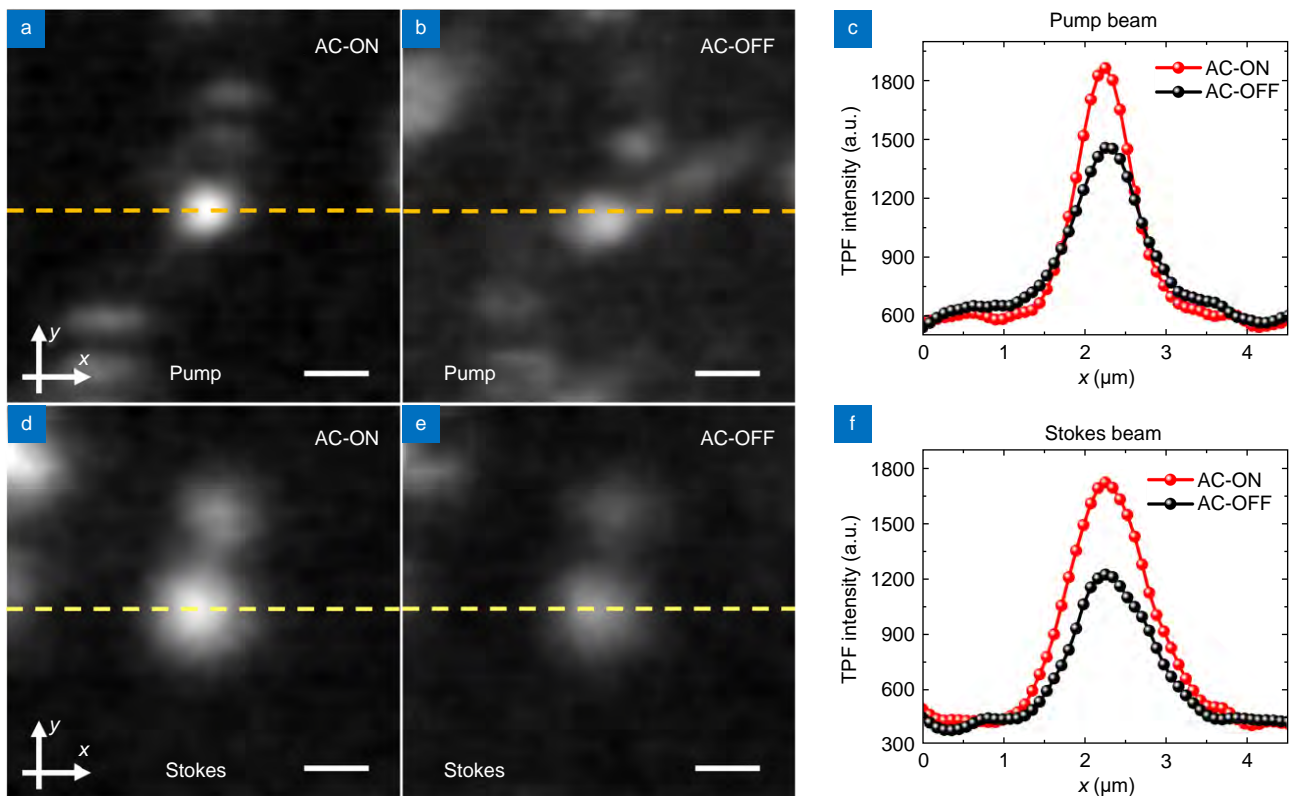


**Fig. S1** | (a, b) TPF images of the 500 nm fluorescent bead captured by pump beam (800 nm) in  $x$ - $y$  plane, corresponding to the conditions of system aberrations correction (AC-ON) and the absence of aberration corrections (AC-OFF). Scale bar: 1  $\mu\text{m}$ . (c) The TPF intensity distribution of fluorescent bead along dashed line in (a–b). (d–e) TPF images of the 500 nm fluorescent bead obtained by Stokes beam (1041 nm) in  $x$ - $y$  plane, corresponding to the conditions of AC-ON and AC-OFF. Scalebar: 1  $\mu\text{m}$ . (f) The TPF intensity distribution of fluorescent bead along dashed line in (d–e).

## Section 2: Relationship between the axial position of the excitation beam and the phase modulation in PC-SRS

Figure S2(a) presents the schematic of an imaging system, where the Fourier plane is the focal plane of the objective lens in object space. The modulated phase projected on the SLM is also located at the position of the Fourier plane. Figure S2(b, c) shows how we control the divergence angle of the incident beams by modulating the phase of the beams on the

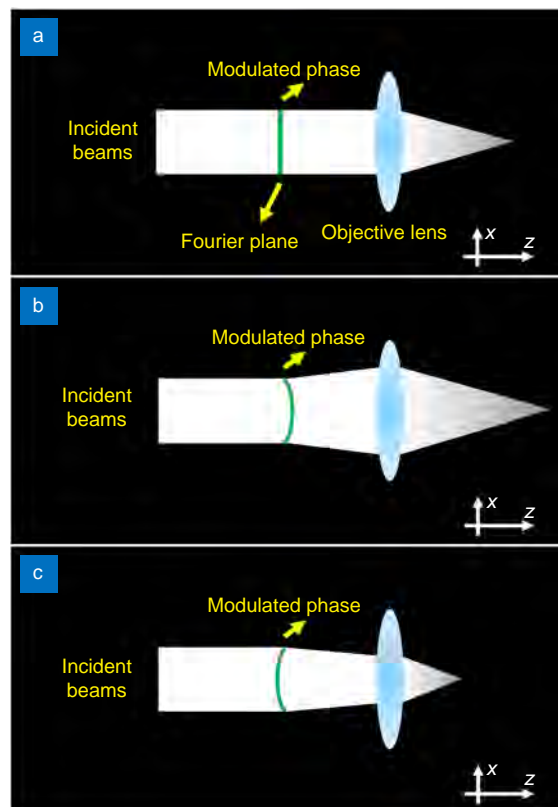


**Fig. S2** | (a) Schematic of an imaging system showing the position of the modulated phase and the Fourier plane. (b, c) Manipulating the axial positions of the focused beams with different modulated phases generated.

SLM, thereby manipulating the axial position of the focused beams in the sample.

### Section 3: Length of the Bessel pump beam in PC-SRS obtained by using TPF imaging on 500 nm fluorescent beads

Figure S3(a) presents the TPF image of 500 nm fluorescent bead excited by the pump beam (800 nm) in  $x$ - $z$  plane. Figure S3(b) shows the intensity distribution of fluorescent bead along the dashed line in (a), in which the length of Bessel pump beam is estimated to be  $4.73\ \mu\text{m}$  by calculating the full width at half maximum (FWHM) of the curve.

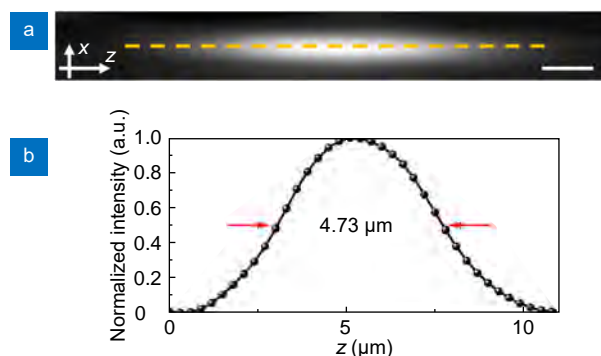
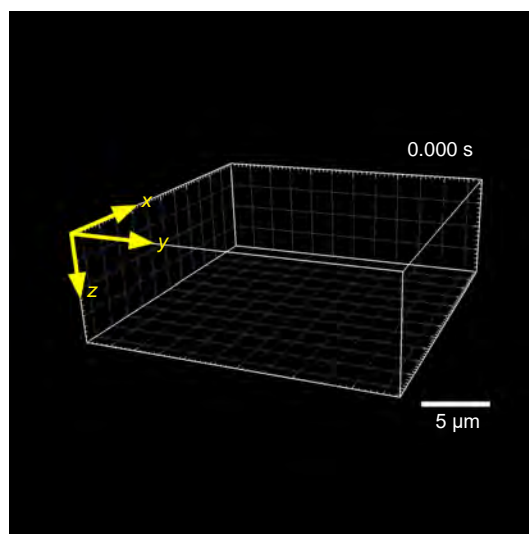


**Fig. S3** | (a) TPF images of the 500 nm fluorescent bead excited by the pump beam (800 nm) in  $x$ - $z$  plane. Scale bar:  $1\ \mu\text{m}$ . (b) The TPF intensity distribution of the fluorescent bead along dashed line in (a). The estimated FWHM of Bessel beam is  $4.73\ \mu\text{m}$ .

### Media for supporting content

**Media S1:** Brownian motion of PS beads (3D SRS at  $2885\ \text{cm}^{-1}$  of  $\text{CH}_2$  asymmetric stretching) in water measured by PC-SRS.  $64 \times 64$  pixels for 2D scanning, axial step size of  $4\ \mu\text{m}$ . Total 4 depths and 77 ms acquisition time for capturing one 3D volume (13 Hz).



**Media S2:** Snapshots of the SRS sectioning images (SRS at  $2935\text{ cm}^{-1}$  ( $\text{CH}_3$  stretching of lipids and proteins) and  $2186\text{ cm}^{-1}$  (CD bond)) with respect to different tissue depths in tumor and normal liver in 6 dpf zebrafish, captured by using PC-SRS.  $256 \times 256$  pixels for 2D scanning, axial step size of  $8.8\text{ }\mu\text{m}$ . Total 9 depths and 15 s acquisition time for capturing one 3D volume.

